horticulturae

MDPI

Article

Study on the Mechanical Properties and the Way of Breaking the Shell of Fresh *Camellia oleifera* Fruit

Xuan Wei [1,2], Xuanqi Chen [1], Peng Liao [1] and Wencheng Huang [1,*]

[1] School of Mechanical and Electrical Engineering, Fujian Agriculture and Forestry University, Fuzhou 350002, China
[2] Fujian Key Laboratory of Agricultural Information Perception Technology, Fujian Agriculture and Forestry University, Fuzhou 350002, China
* Correspondence: hwc@fafu.edu.cn

Abstract: In this study, based on the physical and mechanical parameters of *Camellia oleifera*, the mechanical model of *Camellia oleifera* was rebuilt and analysed to reveal the damage mechanism of fruit shell breakage. The results revealed that under the same conditions (e.g., axial loading form), the stress of the fruit uniformly diffused from the extrusion point to the periphery and depth, and the maximum equivalent stress was 9.4104 Mpa. While under radial loading, the stress of the fruit extended axially along the dorsal line of the tea seed, and the maximum equivalent stress was 6.9467 Mpa. The maximum stress under the two loading modes occurred at the joint between the middle column of the shell and the calyx. The increased loading displacement decreased the stress on the fruit, making it easier to break the shell of *Camellia oleifera* by radial extrusion. The results can serve as a reference for the development of different equipment to break the shell of the *Camellia oleifera* fruit.

Keywords: *Camellia oleifera* fresh fruit; finite element method; stress and strain; shell-breaking rate; tea seed damage

check for updates

Citation: Wei, X.; Chen, X.; Liao, P.; Huang, W. Study on the Mechanical Properties and the Way of Breaking the Shell of Fresh *Camellia oleifera* Fruit. *Horticulturae* **2023**, *9*, 236. https://doi.org/10.3390/horticulturae9020236

Academic Editor: Esmaeil Fallahi

Received: 30 December 2022
Revised: 26 January 2023
Accepted: 7 February 2023
Published: 9 February 2023

Copyright: © 2023 by the authors. Licensee MDPI, Basel, Switzerland. This article is an open access article distributed under the terms and conditions of the Creative Commons Attribution (CC BY) license (https://creativecommons.org/licenses/by/4.0/).

1. Introduction

Tea oil, also known as "Oriental olive oil", is one of the most popular woody edible oils in China and has high nutritional values. The separation of the *Camellia oleifera* (Figure 1) shell and tea seed (Figure 2) is important in the production and processing of tea oil [1]. With the continuous expansion of planting areas and the substantial increase in fresh fruit yield, traditional natural drying and manual shelling can no longer meet the rapid development of the market. A *C. oleifera* shell-breaking device can effectively reduce the breakage rate of tea seeds, greatly improve the efficiency of shell-breaking, and reduce labour intensity and production cost. The structure of the *C. oleifera* shell and fruit is non-uniform and requires both macroscopic and microscopic characterisation for an optimal understanding of the shell-breaking process [2,3]. For full-shell fragmentation and preservation of the inner kernel, a shell-breaking device should be carefully designed and optimised. The structure of the *C. oleifera* fresh fruit is complex [2,3], such that the thickness of the shell and the distribution of the tea seeds are difficult to determine externally. Research on the mechanism of shell breaking and the interaction between fruit and tea seeds is also lacking due to the slow shelling machinery of the *C. oleifera* fresh fruit.

Studies have been conducted to improve the efficiency of fruit shelling and preserve the integrity of the inner kernel. These results indicated that the basic size, moisture content, density, and mechanical properties of shell fruit materials are closely associated with shell-breaking efficiency. Da et al. [4] found that the harvest time of bitter fruits and seeds can be evaluated by size and quality. Huang et al. [5] measured the physical and mechanical properties of different varieties of Dactylis sativus seeds and found that axial shell breaking could effectively reduce the kernel breakage rate. Swami et al. [6] studied the

mechanical properties of cashew nuts (Figure 3a) under compression load with different water content and reported that increasing the water content gradually decreased the rupture force and increased the deformation of cashew nuts. Rasli et al. [7] studied the effects of crop parameters and two loading directions on the mechanical properties of oil palm small fruits (Figure 3b) and found that the breaking force and energy increased with the increase in small fruit mass under two loading directions. The values of fracture force and energy of all mass classes under vertical load were lower than those under horizontal load. Ca'rcel et al. [8] revealed that the hardness and fracture force of pine nut (Figure 3c) shells were negatively correlated with water content, whereas the fracture deformation was associated with the water content, with a maximum value of 1.8 mm. Yang et al. [9] measured the physical parameters and geometric dimensions of chestnuts (Figure 3d) and analysed the loading of chestnuts in different directions. It was found that the beak of the chestnut was easier to deform when the Y direction was along the texture direction of the chestnut material and when there was compression along the Y direction. This made it easier to crack the chestnut shell, which was beneficial to chestnut shelling and provided a theoretical basis for the deep processing of chestnuts. However, the structure of agricultural materials is non-uniform, and the internal dynamic changes of materials are difficult to analyse from the external macroscopic physical characteristics and mechanical tests. Therefore, it is necessary to analyse the stress and strain inside the material to design an effective shell-breaking device. Celik et al. [10–12] studied the mechanical properties of the Bigen fruit (Figure 3e) by explicit dynamic simulation analysis and noted that the top of the suture line of the fruit shell was the weakest point of the whole structure. Cracking at the top of the suture line gradually spread downwards upon loading, which caused plastic deformations of the inner nuts. Cao et al. [13] analysed the stress distribution of walnut under hammer loading with different nest numbers, with seven yielding the best results. Bao et al. [14] verified the goodness of fit (less than 5%) of the walnut (Figure 3f) spherical thin shell model through a texture meter shell-breaking experiment. Through the torque-free theory and finite element simulation, it was found that shell stress had a gradient-decreasing distribution in the load-concentrated force area, and the internal forces were equal in all directions, which provided a theoretical basis for the research and development of shell-breaking equipment. Various parameters and characteristics of shell fruit materials are closely related to shell-breaking efficiency, but the same parameters have different effects on different fruits. For example, shell hardness is associated with shelling rate, but Fornés et al. [15] found that the shell hardness of almonds from the native germplasm of Majorca (Spain) might be an independent variable because of its weak correlation with shelling percentage and nut weight. Hence, it is necessary to study and analyse the physical parameters, mechanical properties, and internal stress and strain of shell fruits to improve the hulling efficiency and the integrity of internal kernels.

China is rich in *C. oleifera* fruit; by the end of 2020, the planting area of *C. oleifera* in China was predicted to reach 4533 khm^2, high-yield *C. oleifera* forests were expected to reach 933 khm^2 in area, and the output of *C. oleifera* was expected to reach 627 kt [16]. However, the shelling process is inefficient due to the lack of corresponding machinery and equipment. By systematically studying the physical and rheological mechanical properties of fresh *C. oleifera* fruit, the whole process of tea oil production can be improved to ensure a cost-saving and efficient production and promote a sustainable and stable *C. oleifera* industry. In this paper, a model of the *C. oleifera* fresh fruit was established by reverse engineering technology. The shell-breaking process of the *C. oleifera* fruit was then simulated and analysed based on the finite element method. The findings from this study can provide a reference for the design of a shell-breaking device for *C. oleifera* fruits.



Figure 1. High-yield *Camellia oleifera* trees growing in hilly and mountainous areas.

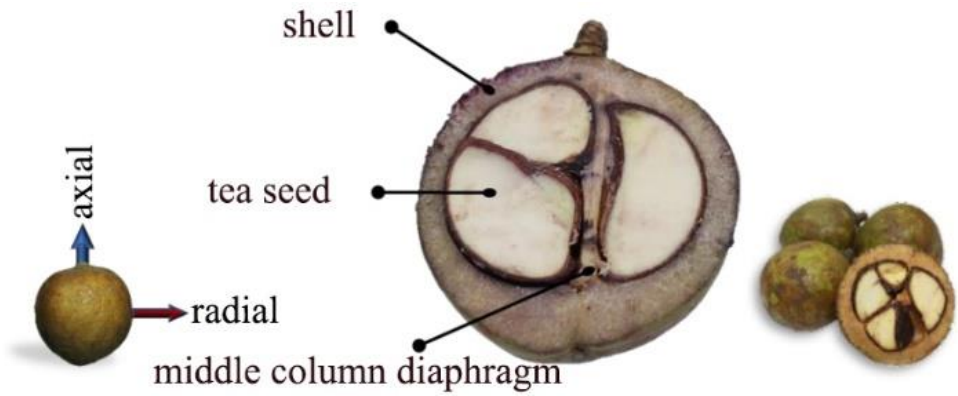

Figure 2. The cross-sectional view of fresh *Camellia oleifera* fruit.

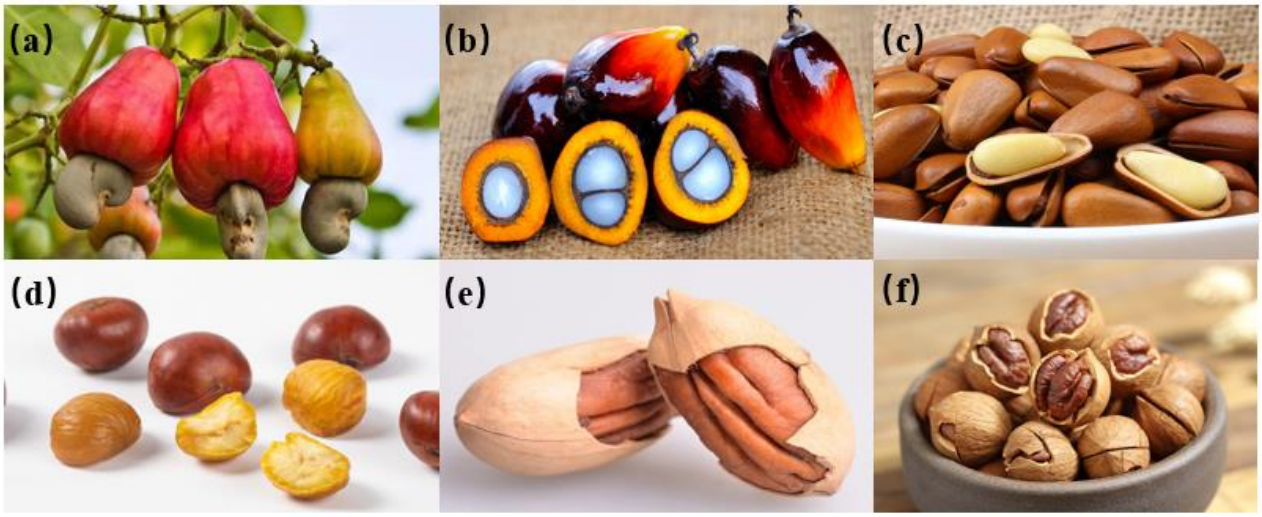

Figure 3. Some breaking fruits (**a**) Cashew nuts. (**b**) Oil palm small fruits. (**c**) Pine nut. (**d**) Chestnuts. (**e**) Bigen fruit. (**f**) Walnut.

2. Materials and Methods

2.1. Camellia oleifera Fruit Samples

Fresh *C. oleifera* fruits were collected from a Tongkou-State-owned forest farm in Minhou County, Fuzhou City, Fujian Province, in November 2020. The 120 selected *C. oleifera* fruits were vacuum-packed with a vacuum extractor (BD-B1, Yongkang Shiguang Electronics Technology Co., Ltd., Jinhua, China) and transported to the laboratory in a constant temperature and humidity incubator (HSP350B, Shanghai Kuntian Test Instrument Co., Ltd, Shenyang, Liaoning Province, China) for storage. The temperature was set to 0–5 °C, and the humidity condition was 85%.

2.2. Determination of Physical Parameters of Camellia oleifera Fruit

The physical parameters of 100 *C. oleifera* fruits were measured randomly. The axial and diameter lengths of each fruit were measured with a digital vernier calliper (MNT-150T, Germany MNET, precision 0.01 mm), and the weight of the fruits was ascertained with an electronic scale. The fruit was broken along the axial direction by using a high-performance electric mill (DREMEL 4000 Robert Bosch Tool Corporation, Stuttgart, Germany), and the thickness of the shell in the calyx, waist, and pedicle and the maximum size of tea seeds were also measured. The total weight of the tea seed in a single fruit was obtained by electronic scale, and the proportion of fruit shell seed was calculated by Equation (1):

$$\gamma = \frac{m - m_1}{m_1} \quad (1)$$

where γ is the specific gravity of shell seed, m is the total weight of a single Camellia fruit (g), m_1 is the weight of the tea seed in a single fruit (g). The cross-section of a fresh *C. oleifera* fruit is illustrated in Figure 2. The water content of the fruit was measured according to GB/T20264 (determination of water content of grain and oil by secondary drying), and the density values of the whole fruit, shell, and tea seed were measured by the drainage weighing method [17].

2.3. Microstructure Observation

To study the internal structure of the *C. oleifera* fruit, the axial and radial sections of the calyx, waist, pedicle, and seed shell of the fruit were sliced and placed in an ion spraying sputtering instrument (JFC-1600, JEOL, Akishima, Tokyo, Japan). After vacuum extraction, the samples were sprayed with gold for 2 min. The sample was then fixed with conductive adhesive on a scanning electron microscope (TM3030, Hitachi, Qingpu District, Shanghai) and observed.

2.4. Obtaining Mechanical Parameters of C. oleifera Fruit

The whole fruit and seeds of *C. oleifera* were compressed by a universal testing machine (Shimadzu AG-X plus, Suzhou, China) to determine the shelling force and elastic modulus of the fresh fruit. Fifteen fresh fruits with an outer diameter of 30–40 mm were randomly selected and divided into three groups, with five samples in each group. According to Celik et al. [11], the static compression speed was set to 5 mm/min, and the three groups were subjected to axial compression, radial compression, and tea seed compression until the shell and tea seed broke. The force–displacement curves of fresh fruits and tea seeds in the compression process were recorded in real time by the data acquisition system. The elastic modulus of the *C. oleifera* fruit was calculated with Equation (2):

$$E = \frac{3F\left(1 - \mu^2\right)}{4D^{\frac{1}{2}}\rho^{\frac{1}{2}}} \quad (2)$$

where E is the elastic modulus of fruit (MPa), F is the applied shell-breaking force (N), D is the deformation (mm), P is the curvature radius of the material (mm), and μ is Poisson's ratio of the materials. Shell-breaking force and deformation were calculated via

the compression test. The radius of curvature was measured by the radius of the curvature meter. The Poisson's ratio of agricultural materials ranges from 0.3 to 0.5, such that the greater the brittleness of the materials, the smaller the Poisson's ratio. In this experiment, the Poisson's ratio of tea seeds was 0.3, and that of fruit shells was 0.4. The measurements taken were similar to the compression test of the Bigen fruit by Celik et al. [10–12].

2.5. Three-Dimensional Solid Modelling of Camellia oleifera Fruit

Establishing a three-dimensional model is the premise of finite element analysis, and the rationality and accuracy of the model are related to the results and speed of the finite element solution. In this study, reverse engineering technology was used for accurate modelling. In Figure 4, the point cloud data, with internal complex structural positional relations, are obtained by an industrial structured light scanner (Techlego T5, TECHLEGO (TIANJIN) CO., LTD, Xiqing District, Tianjin, China). The scanner had a resolution of 131 w pixels, a single frame accuracy of 0.007 mm, and a measurement point distance of 0.06 mm. The fruits were placed on an automatic rotating table and observed every 15°.

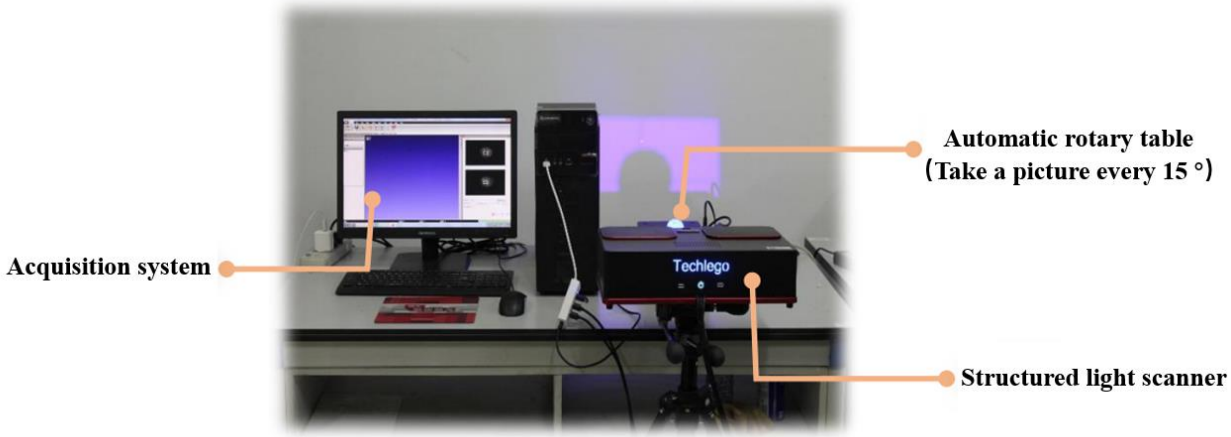

Figure 4. Laser positioning non-contact surface scanner.

The point cloud data of the *C. oleifera* fruit were imported into the Geomagic studio software. After removing the isolated points outside the body and non-connected points, the triangle network was encapsulated and reduced by using the "simplification" command. Burrs and nails on the surface of the model were removed by using the "removal" and "elimination of nails" commands for a smoother model. After the model was imported into Geomagic DesignX, the solid model could be formed directly. The solid models of tea seed and shell after positioning are depicted in Figure 5a,b. To reduce the time and memory of subsequent simulation calculation, the reverse file was imported into the 3D modelling software SolidWorks 2021, the shapes of fruit shells and tea seeds were extracted by spline curve operation, and the simplified model of the fresh fruit was obtained by feature rotation (Figure 5c,d).

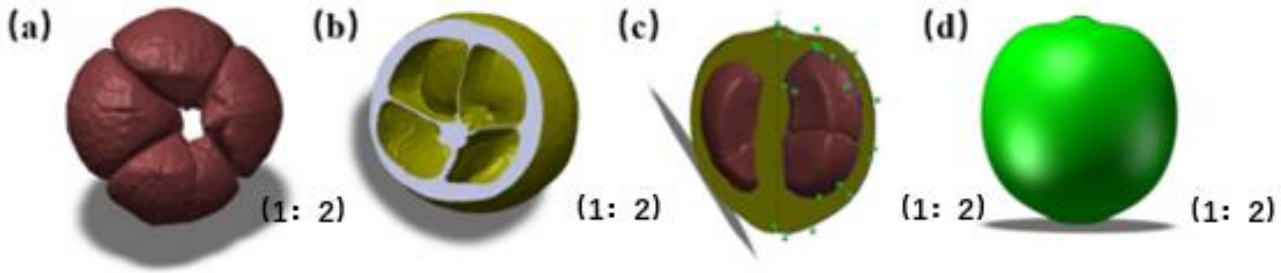

Figure 5. Solid model and model simplification of the *Camellia oleifera* fruit. (**a**) *Camellia* seed model. (**b**) Shell model. (**c**) Spline curve extraction. (**d**) Simplified fruit model.

2.6. Finite Element Dynamic Analysis

In the ANSYS Workbench 2021 R1 software (ANSYS Corporation, Canonsburg, PA, USA), with the use of the Explicit Dynamics module in the Analysis Systems module group, the parameters and models of the *C. oleifera* fruit were input, and structural steel was selected as the upper and lower extrusion steel plate material to perform the dynamic simulation. The smooth waxy surface of the fresh *C. oleifera* fruit facilitated the transfer of tea seeds into the fruit, with frictionless surface contact. The grid size of the fruit shell and tea seed was 5 mm. The steel plate was automatically divided into hexahedral mesh by the software, and the number of nodes and elements of the model were 9835 and 9441, respectively. During the setting of the boundary constraint conditions, the object needed higher relative motion speed due to the short time of explicit dynamics calculation. Hence, the initial motion speed of the upper steel plate was set to 10,000 mm/s. Considering that the steel plate will rebound after pressing down at a uniform speed under actual working conditions, the downward speed of the steel plate was set to 10,000 mm/s for constant movement stability. Therefore, the analysis time step was set to 0.001 s when the steel plate moved down by 10 mm.

3. Results and Discussion

3.1. Physical Parameters of Fresh Camellia oleifera Fruit

The statistical results of the physical parameters of fresh *C. oleifera* fruit are reported in Table 1. The axial and diameter lengths of fresh fruits were 23.20–56.20 mm and 21.90–56.30 mm, respectively. The thickness of the waist, pedicle, and calyx had average values of 5.48 mm, 3.90 mm, and 8.54 mm, respectively. The maximum size of the tea seeds ranged from 13.59 mm to 30.45 mm. The whole fruit mass ranged from 5.93 g to 65.19 g, and the tea seed mass ranged from 1.75 g to 28.53 g. The average values of whole fruit mass and tea seed mass were 26.05 g and 9.74 g, respectively. In terms of shell–seed specific gravity data, there were significant differences in shell–seed mass ratio between different fruits because the shell of *C. oleifera* is controlled by independent genes in the growth process. The moisture contents of the whole fruit, shell, and seeds were 60.66%, 73.00%, and 44.55%, respectively. The density of the whole fresh fruit and shell of *C. oleifera* was 1.04 g/cm^3. The density of tea seeds was slightly higher at 1.32 g/cm^3; this higher density may be caused by the different contents of oil and protein in tea seeds, and the different degree of binding of various substances in tea seeds. The experimental results were relatively similar to those reported by Lan Feng et al. [17].

Table 1. Statistical table of parameters of physical characteristics of fresh *Camellia oleifera* fruit.

Category	Index	Minimum	Maximum	Average	Moisture Content (%)	Density (g/cm^3)
Fruit	Shaft length (mm)	23.20	56.20	35.50 ± 5.92 *	60.66 ± 4.75	1.04 ± 0.03
	Diametral length (mm)	21.90	56.30	36.50 ± 6.74		
	Quality (g)	5.93	65.19	26.05 ± 13.27		
Shell	Peduncular thickness (mm)	2.42	9.91	5.48 ± 1.41	73.00 ± 0.78	1.04 ± 0.12
	Lumbar thickness (mm)	1.79	7.66	3.90 ± 1.07		
	Calyx thickness (mm)	4.16	15.00	8.54 ± 2.25		
Tea seed	Seed length (mm)	13.59	30.45	21.35 ± 3.19	44.55 ± 4.27	1.32 ± 0.17
	Seed weight (g)	1.75	28.53	9.74 ± 5.57		
Specific gravity of shell and seed		0.93	2.97	1.90 ± 1.07	— —	— —

Note: * The values in the table are mean ± standard deviation.

3.2. Observation on the Microstructure of Fresh Camellia oleifera Fruit

3.2.1. Microscopic Scanning Results and Analysis of Fruit Shells

Figure 6 displays the microstructure of the calyx, waist, and pedicle of the *C. oleifera* shell. Vascular tissue is composed of mainly phloem, xylem, and microtubules and is important for the nutrient supply and skeletal structure. From the cross-section (Figure 6a) and longitudinal section (Figure 6b), a large number of vascular bundles were gathered in the pedicle, and the outside of the vascular bundles was wrapped and protected by parenchyma. The smallest unit of the vascular bundle group was the microfilament, and many microfilaments formed the vascular tissue in a spiral conformation. The vascular tissue was regularly arranged in clusters in a certain way, and the outermost layer was wrapped by parenchyma and extended outward, which was consistent with the observations by Wang et al. [2]. There were no obvious stone cells in the pedicle.

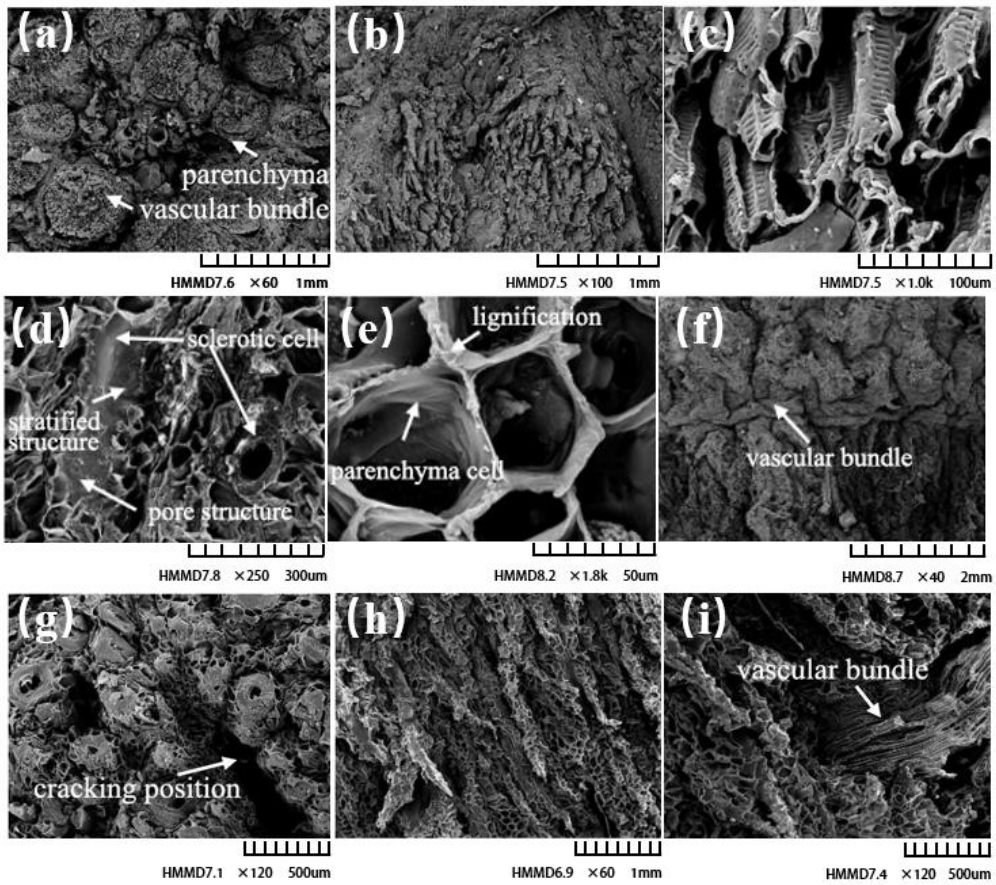

Figure 6. Scanning electron microscopic observation of fruit shell. (**a**) Cross-section at fruit pedicle (60, 1000 μm). (**b**) Longitudinal section at fruit pedicle (100, 1000 μm). (**c**) Vascular structure at fruit pedicle (1000, 100 μm). (**d**) Cross-section at the waist (250, 300 μm). (**e**) Longitudinal section at the waist (18,800, 50 μm). (**f**) Vascular structure at the waist (40, 2000 μ m). (**g**) Cross-section at calyx (120, 500 μm). (**h**) Longitudinal section at calyx (60, 1000 μm). (**i**) Vascular structure at calyx (120, 500 μm).

Figure 6d,e show the cross-section and longitudinal section of the waist of the shell, respectively. Distinct from the pedicle, the stone cells in the waist were embedded in parenchyma cells, and the number increased in comparison to the pedicle. Most were short and spindle shaped, with obvious pore characteristics and a rich hierarchical structure. Stone cells have thick layered cell walls and mesoporous structures, which are responsible for the structural strength of fruit shells and the material exchange between the inside and outside of fruits [3,18,19]. The structure of parenchyma cells was closely arranged in a honeycomb shape, which could effectively alleviate the external impact. Due to the overlap and proliferation of cells, the intercellular complex layer and cell corner of

adjacent parenchyma cells showed slight lignification, which could be beneficial for the reinforcement between cells. The tufted vascular tissue at the pedicle passed through the shell structure at the waist and extended to the calyx (Figure 6f).

Figure 6g,h display the microstructure of the calyx in the transverse and longitudinal sections. The cracking of the calyx started from the inside, and there were abundant stone cells neatly arranged on both sides of the cracking site. These stone cells were slenderer than those at the waist. The cracking shape of the calyx was straight. The structural strength of the stone cells was higher than that of the parenchyma cells. The parenchyma tissue broke during fruit compression and continued to tear along the transverse and longitudinal directions, with the fruit shell finally cracking in the calyx. The vascular bundle was connected to the ovary at the calyx and transported nutrients inwards (Figure 6i).

3.2.2. Microscopic Scanning Results and Analysis of Seed Shell

Figure 7 displays the microstructure of the seed shell surface under an electron scanning microscope. Stone cells are the main constituent cells of seed shells, which form a layered structure through tight bonding. The stone cell layer is divided into inner and outer layers, which are arranged vertically with each other. The surface seed shell is composed mainly of a large number of short, rod-shaped and spindle-shaped stone cells that are closely bonded to form a highly compact protective structure. The pore in this protective structure is very small and is only used for material exchange between the tea kernel and the outside. The lignin in the seed shell exists mainly inside and outside of the cell wall, which fills the gaps between the stone cells to form a shell with extremely high density [20,21]. In Figure 7c, the seed shell breaks occurred at the junction between the cells and spread to the nearby junction.

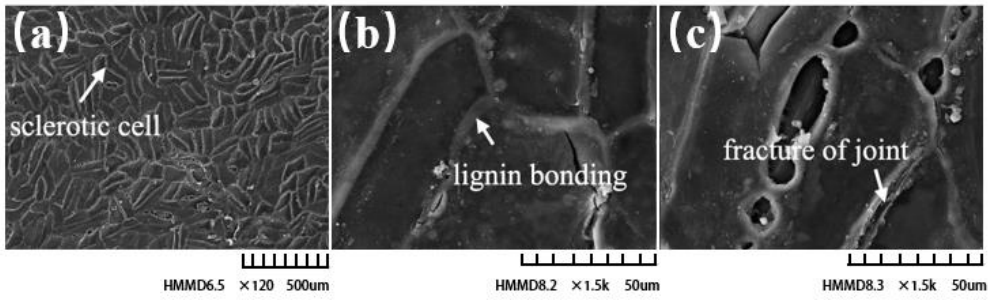

Figure 7. Scanned electron microscopic observation of seed shell. (**a**) Transverse section of seed shell (120, 500 μm). (**b**) Longitudinal section of seed shell (1500, 50 μm). (**c**) Seed shell rupture (1500, 50 μm).

3.3. Mechanical Properties of Fresh Camellia oleifera Fruit

The axial and radial compression load-displacement curves in Figure 8a,b are convex to the displacement coordinate system in the initial stage, which could be due to the high moisture content in the material. This applied large shear strain in the material under compression, which is common for fresh agricultural materials. The differences in load and displacement at the rupture point of samples were the thickness of the pedicle, waist, and calyx and the distribution and size of tea seeds. In addition, the distribution of vascular tissues was inconsistent, which led to the difference in load and displacement at the rupture point of the samples. Both the fruit and tea seed compression curves (Figure 8c) exhibited an elastic stage, breaking points, and a sudden stress drop during cracking, which implied that both fruit and tea seed comprise elastic materials. From the comparison of mechanical characteristic curves of different parts (Figure 8d), the compression curves of the axial shell, radial shell, and tea seed were similar in shape, but there were differences in mechanical parameters such as shell-breaking force, shell-breaking point position, and elastic modulus. The average load and displacement of the fruit-shelling point under axial compression

were greater than those under radial compression, which was mainly affected by shell thickness, tea seed slip, and fruit microstructure (Table 2).

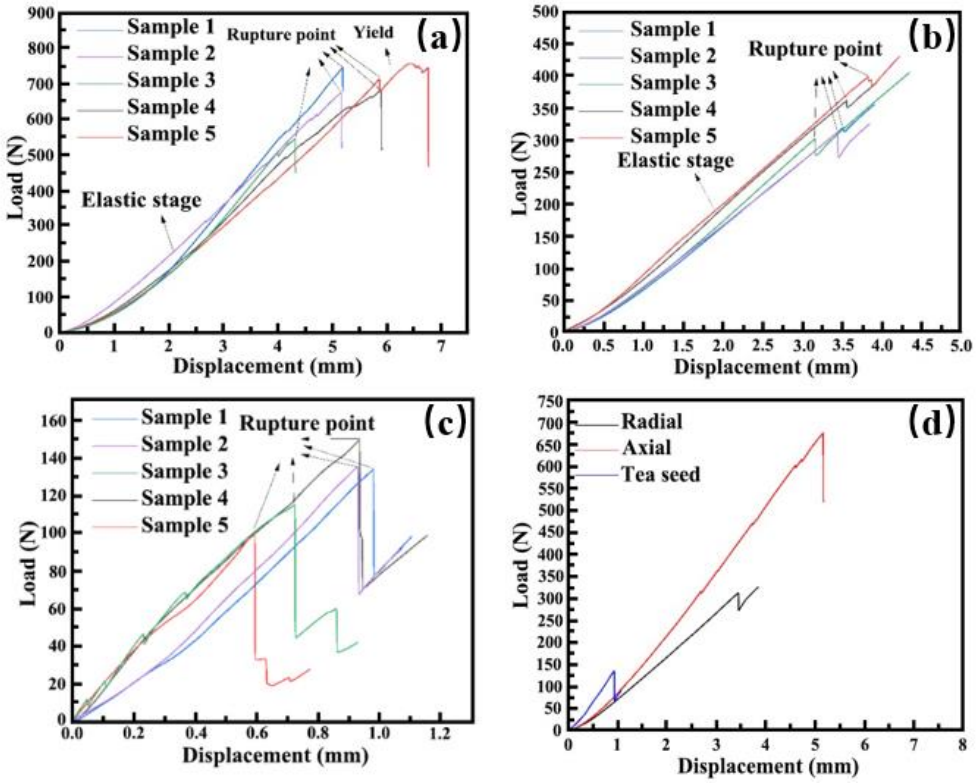

Figure 8. Load-displacement curves of fresh *Camellia oleifera* fruit. (**a**) Axial compression load-displacement curve. (**b**) Radial compression load-displacement curve. (**c**) Compression load-displacement curve of tea seed. (**d**) Comparison of mechanical characteristic curves of different parts.

Table 2. Mechanical properties of fresh *Camellia oleifera* fruit.

Index	Displacement of Shell-Breaking Point (mm)	Shell-Breaking Force (N)	Elastic Modulus (Mpa)	Cross-Sectional Area (mm^2)	Compressive Strength (Mpa)
Axial	5.29 ± 0.58 *	671.18 ± 67.95	12.03 ± 1.15	306.62 ± 64.43	2.19 ± 0.42
Radial	3.50 ± 0.21	338.26 ± 35.94	11.13 ± 0.81	438.56 ± 65.80	0.77 ± 0.13
Tea seed	0.83 ± 0.15	126.60 ± 17.01	38.87 ± 7.12	74.63 ± 5.29	1.70 ± 0.20

Note: * The values in the table are average ± standard deviation.

Table 2 highlights the mechanical properties of fresh *C. oleifera* fruit. The shell-breaking force of the *C. oleifera* fruit under radial compression was 338.26 N, which was about half of that under axial compression. This was justified by the physical parameters of fresh *C. oleifera* fruit and the microscopic scanning results of the shell. Compared with the waist of the shell, the shell of the pedicle and calyx was thicker, thereby requiring more shell-breaking force. Moreover, the shell accumulated a large number of vascular bundles in the pedicle, which were wrapped and protected by parenchyma to alleviate the external impact. The joint action of the two factors reduced the shell-breaking force under radial compression. According to the research results of Lan Feng et al. [17], the axial breaking force of tea fruit with an outside diameter in the range of 30–40 is about 430 N, which is caused mainly by the following factors. Firstly, the density of the tea fruit, fruit shell, and tea seed measured in this paper is slightly higher than that measured by Lan Feng et al. Because of the different growth environment of tea fruit, the pressure required for shell breaking is increased due to the higher density. Secondly, the thicker Camellia fruit used

in this research would have also increased the force required for shell breaking. At the same time, the different degree of binding of substances in different Camellia fruit further affects the strength of shell breaking. The shelling force of tea seeds was 126.60 N. The rupture point of axial compression was deeper than that of radial compression due to the thicker shell of the pedicle and calyx. The thicker shell could not crack at once during the rupture process, and the internal shell fibre was continuously torn during the rupture process. Hence, complete cracking could occur only when the axial compression reached a larger displacement. The displacement required for tea seeds to reach the rupture point was 0.83 mm. Due to the influence of breaking force and displacement of the breaking point, the difference between axial and radial modulus of elasticity was small. In the experiment, the cross-sectional area of the *C. oleifera* fruit shell was different when it was cut in different directions. According to the physical parameters, the thickness of the shell at the waist is the smallest; thus, the cross-sectional area cut along the radial direction is the smallest, and the structure is weak, which leads to the low compressive strength of the fruit under radial loading. Therefore, there is a big difference in the compressive strength of the fruit under different directions of loading, and the compressive strength under axial loading is 2.19 Mpa. Radial loading is only 0.77 Mpa; thus, it is necessary to ensure that the shell is broken and the seeds are not damaged.

3.4. Simulation Result Analysis

Fresh *C. oleifera* fruit and tea seed materials are not commonly used as engineering materials. The rheological properties of fresh *C. oleifera* fruit shell and tea seed are defined as isoelastic materials, with an elastic modulus of 12.03 Mpa, a Poisson's ratio of 0.4, and a density of 1040 kg/m^3. The elastic modulus of tea seed was 38.87 Mpa, the Poisson's ratio was 0.4, and the density was 1320 kg/m^3.

3.4.1. Analysis of Simulation Results of Axial Extrusion of Intact Fruit

In Figure 9, the nephogram of displacement diffused evenly from the extrusion point to all directions, and there was no deviation. The maximum deformation of the fruit under axial loading was 10.002 mm at the place where the fruit was pressed against the upper steel plate. The analysis revealed that a large number of vascular bundles were gathered in the pedicle of the fruit shell, and stone cells were not observed. Thus, the fruit shell had weaker structural support to resist mechanical damage. However, stone cells were observed in the waist and calyx of the shell, so the deformation of the waist and calyx of the shell was small, whereas the deformation around the calyx of the shell lacking stone cells was large. In addition, under the two-phase extrusion between the steel plate and the top of the tea seed, the shell at the contact position was significantly extruded, resulting in maximum deformation between the fruit and the upper steel plate. Because the lower plate was fixed, the movement of the calyx of the fruit at the lower plate was limited, and stone cells in the calyx of the fruit shell were abundant. This provided good structural strength for minimum deformation between the lower plate and fruit.

From the stress change diagram of the whole fruit under axial loading in Figure 10, the internal stress of the fruit gradually diffused from the loading point to the surrounding area during the loading process. With the increase in the displacement of the upper steel plate, the stress near the extrusion centre point increased and diffused, indicating that the stress had shifted to the extrusion centre point and the maximum stress was greater than 2.0912 MPa. Although the stress change of the fruit diffused outwards, the external stress of the fruit decreased. In addition, the external stress of fruit generally decreased to the range of 1.0456–2.0912 MPa, mainly because the stress gradually changed between the internal tea seed and the shell.

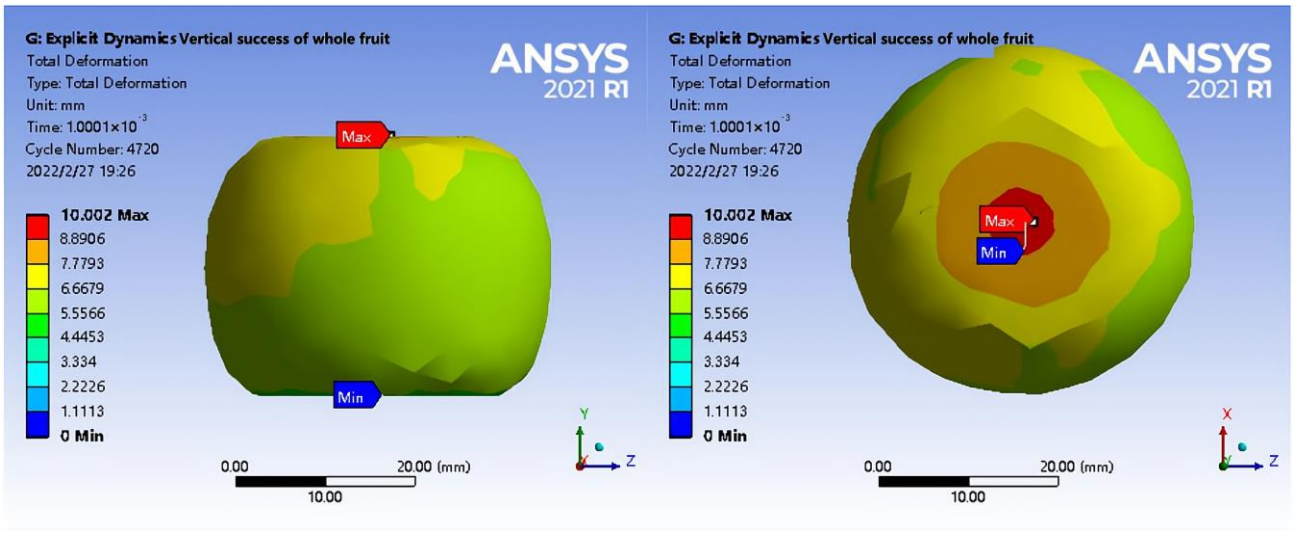

Figure 9. Total deformation diagram under axial loading.

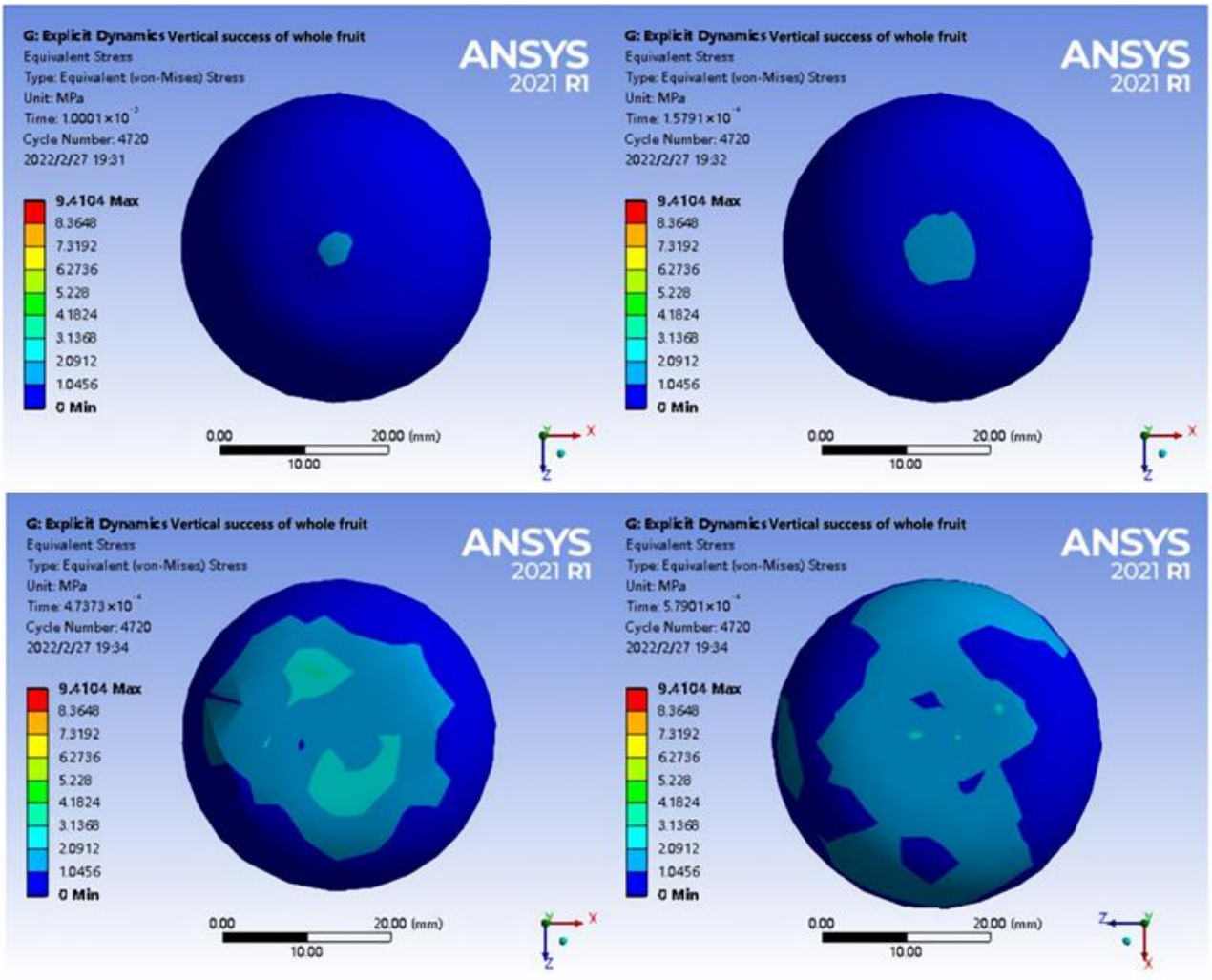

Figure 10. Stress change diagram of intact fruit under axial loading.

3.4.2. Analysis of Simulation Results of Axial Extrusion Half-Section of Complete Fruit

To further evaluate the interaction between tea seeds, shell pillars, and calyx, a stress change diagram after the loading was half-sectioned was obtained (Figure 11). The half-section view of axial loading indicated that the stress near the centre point of extrusion was the contact position between the top of the tea seed and the shell. In addition, when tea seeds were compressed, the stress built up at the junction between the stellar shell and the calyx, and with further compression, the maximum stress was attained at the junction between the stellar shell and the calyx. According to the analysis, the vascular bundles were distributed in the middle of the suture shell, penetrating the whole fruit from the pedicle to the calyx. The outside of the vascular bundles was protected by parenchyma, providing additional structural support. Therefore, part of the load exerted around the pedicle was transmitted to the calyx of the fruit. At the same time, in the macroscopic structure, the displacement from the lower ends of the left and right tea seeds to the middle resulted in intense pressure at the junction between the central column and the calyx of the shell. Meanwhile, the radial displacement of the shell increased, and the junction between the central column and calyx was pulled with a maximum stress of 9.4104 Mpa.

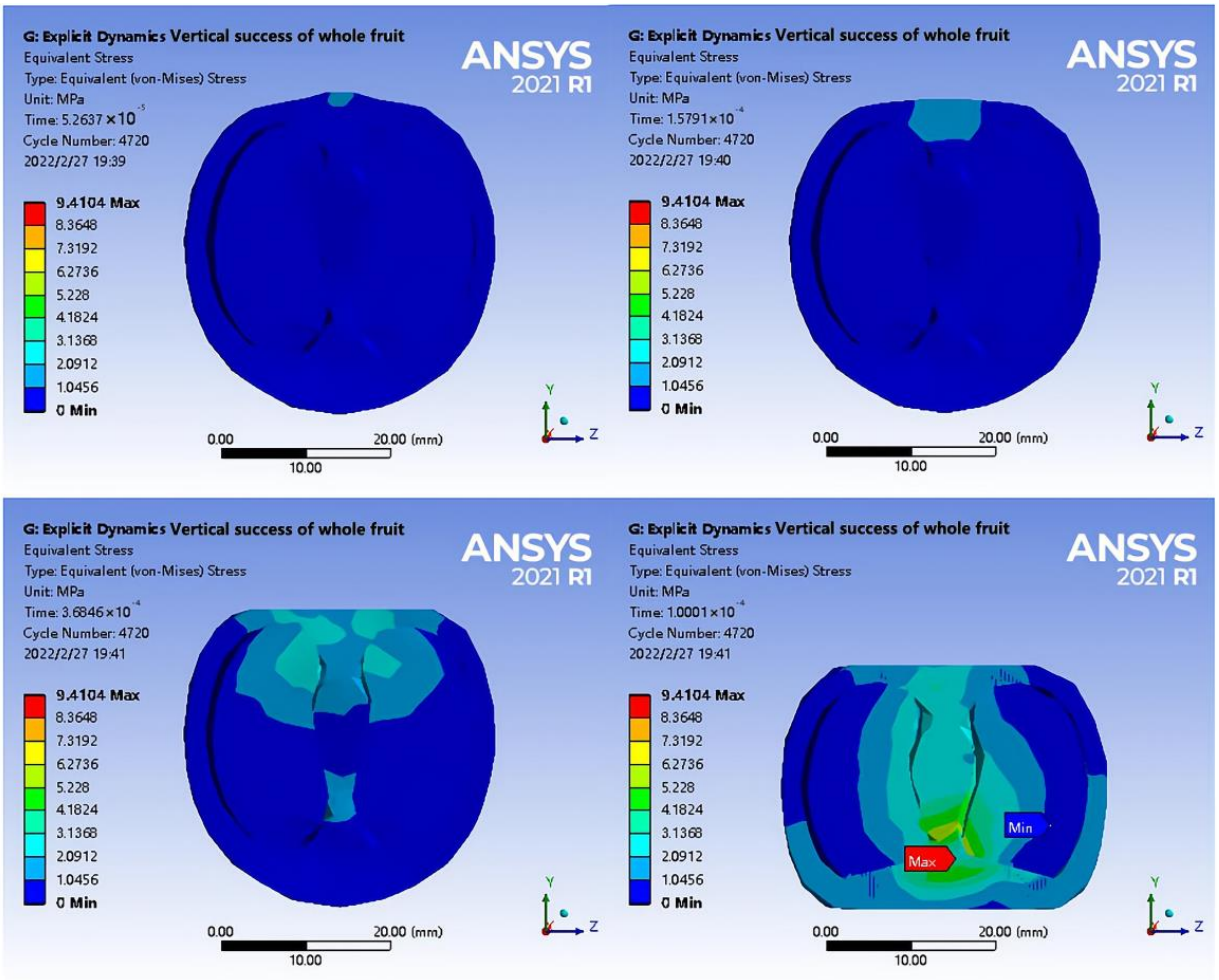

Figure 11. Axial loading stress change diagram of half-section fruit.

3.4.3. Analysis of Simulation Results of Radial Extrusion of Intact Fruit

In Figure 12, the maximum deformation position of the fruit under radial loading occurred at the extrusion position of the upper steel plate, where the maximum deformation reached 10.177 mm. Compared with axial loading, the lateral displacement of non-extrusion under radial loading was relatively smaller. By comparing the cross sections of axial and radial loading and analysing the scanning results of the microstructure, the pedicle and

calyx of the shell, which had a certain resistance to deformation, were thicker in the direction of non-extrusion under radial loading. Secondly, abundant stone cells were observed in the microstructure of the calyx of the shell. In addition, the shell–seed gap between the shell and tea seeds grew larger during axial extrusion, resulting in the appearance of lateral displacement under axial loading than that under radial loading. Under radial loading, the bottom of the shell was limited, and the minimum deformation occurred at the pedicle of the fruit that was in contact with the lower steel plate.

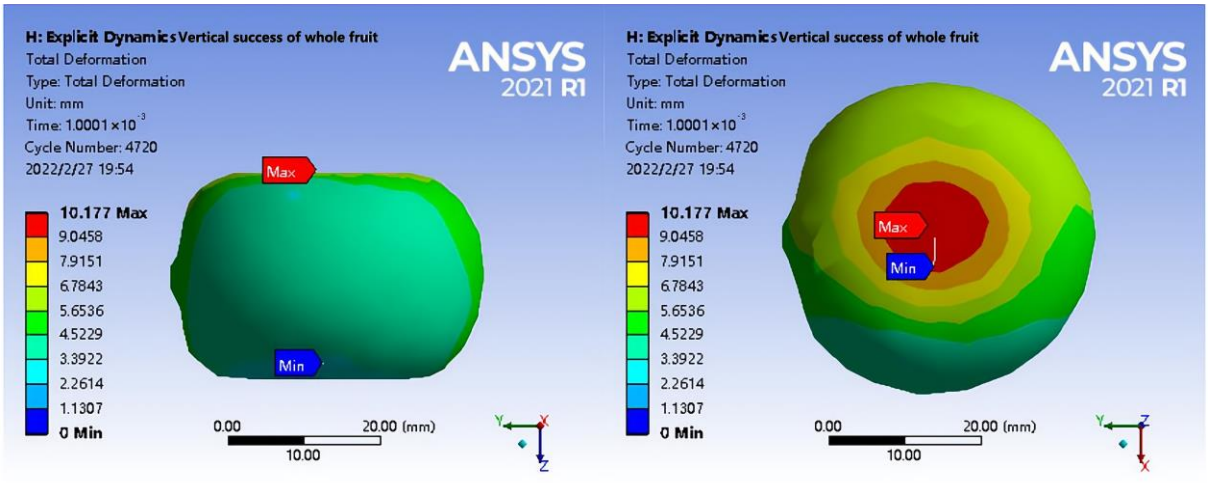

Figure 12. Total strain diagram under radial loading.

In Figure 13, the internal stress of the fruit gradually diffused in the longitudinal axis direction from the loading point during the loading process, which was different from the performance of axial loading. The analysis indicated that the thickness of the shell at the waist was small, and the loading force could be quickly transmitted to the tea seed when the steel plate was extruded. The back of the tea seed was close to a 1/4 spherical curved surface, and the dorsal line was in contact with the shell during extrusion, extending along the axial direction. In addition, the main constituent cells of the seed shell were stone cells. The adhesion between cell walls was weaker than the breaking force of the stone cells themselves, and diffusion occurred at the nearby joint, distributing the stress in the axial direction.

3.4.4. Analysis of Simulation Results of Radial Extrusion Half-Section of Complete Fruit

In Figure 14, the compression stress was transmitted along the extrusion point from the outer shell to the tea seed and middle column due to the small thickness of the waist of the shell. With the support and extrusion of the relative positions of the upper and lower tea seeds, the stress in the abdomen of the tea seed initially increased and diffused to both ends behind the tea seed. As was the case for axial loading, the surface shell had high compactness and structural strength and was affected by the two-phase extrusion of tea seeds and longitudinal deformation of the shell at the junction between the middle column and the calyx. In addition, the diameter was the smallest, and the structure was the weakest, resulting in a maximum stress of 6.9467 Mpa. The longitudinal displacement of the shell increased the gap between the shell and seed, and the two ends of the tea seed were not affected by the load. The simulation data are shown in Table 3.

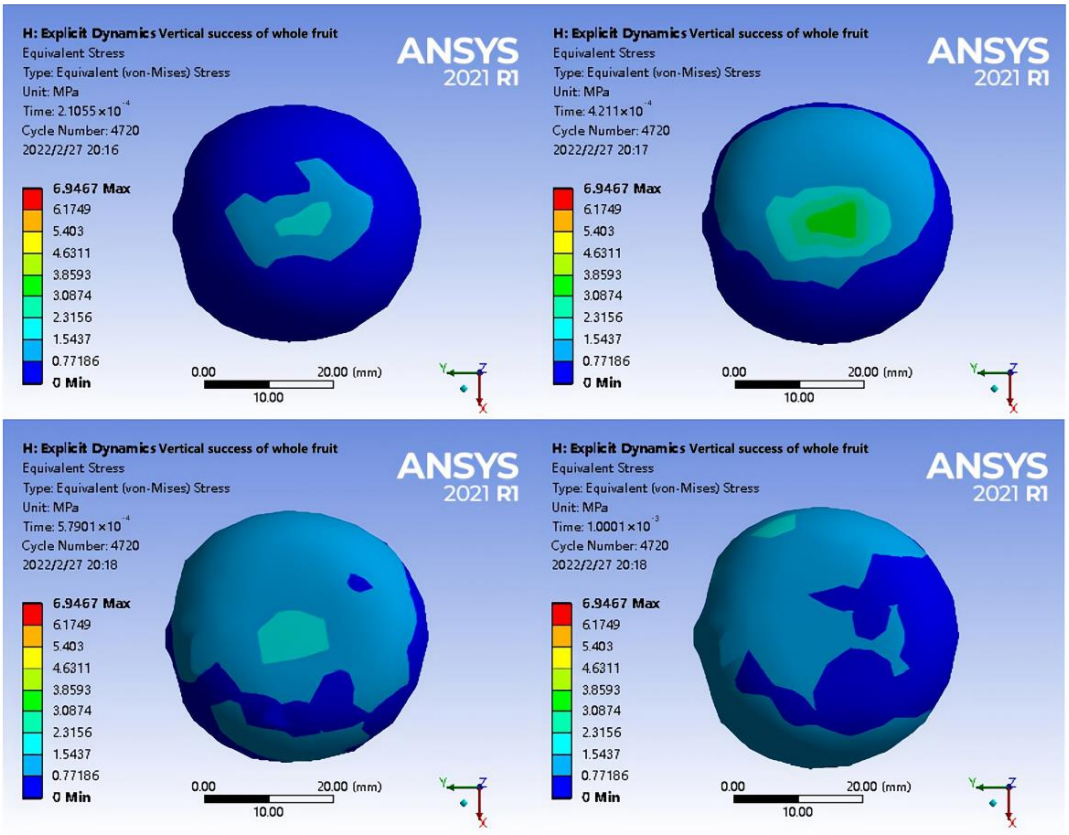

Figure 13. Radial loading stress change diagram of intact fruit.

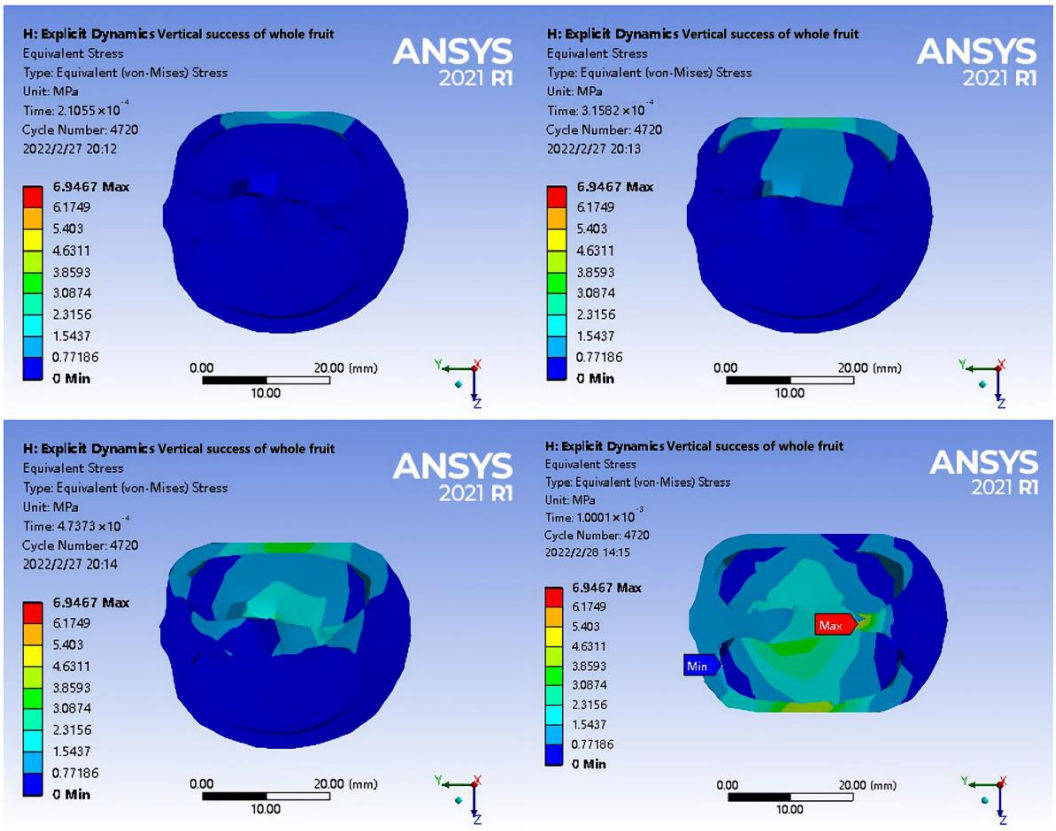

Figure 14. Radial loading stress change diagram of half-section fruit.

Table 3. Extrusion simulation results of fresh *Camellia oleifera* fruit.

Index	Position	Maximum Deformation (mm)	Maximum Stress Value (Mpa)
Axial	External Inside	10.002 — —	2.0912 9.4104
Radial	External Inside	10.177 — —	3.8593 6.9467

After considering the stress performance of the fruit under axial and radial loadings, as well as the physical parameters, mechanical properties, and microstructure of the fresh *C. oleifera* fruit, the fruit shells were easier to break under radial loading. This was due to several reasons. Firstly, the average thickness of the shell at the waist was less than that of the pedicle and calyx. The smaller thickness allowed a quicker transfer of the load to the inner tea seeds under radial loading, whereas that of the back of the tea seeds was close to 1/4 of the spherical curved surface along the axial direction. The tea seeds were able to slide easily and could be better separated from the shell whilst maintaining the integrity of the tea seeds. On the contrary, axial loading compacted and compressed the tea seeds with the shell, damaging the tea seeds in the process. Secondly, the vascular bundles were interspersed in the whole shell axially, and the parenchyma and stone cells supported the structure of the shell. With axial loading, the shell-breaking force reached 671.18 ± 67.95 N, which was twice that of radial loading. Hence, radial loading is a more favourable loading method for shell breaking.

4. Conclusions

In this study, the physical and mechanical parameters of fresh *C. oleifera* fruits were measured, and the microstructure of the fruit was observed by scanning electron microscopy. The stress–strain change and the damage mechanism of the *C. oleifera* fruit shell rupture under different loading conditions were studied by using reverse engineering technology and the finite-element explicit dynamic analysis method. The results reported that the breaking force of fruit under axial loading was 671.18 ± 67.95 N, whereas that under radial loading was only 338.26 ± 35.94 N. The maximum deformation of the fruit under radial loading and axial loading was 10.177 mm and 10.002 mm, respectively. Under the same conditions, the transverse displacement under radial loading was greater than that under axial loading. The influence of the fruit structure and stress transfer mode led to the maximum stress in different loading directions at the junction of the shell column and calyx, and the maximum equivalent stress under axial loading and radial loading were 9.4104 Mpa and 6.9467 Mpa, respectively. The stress of the fruit under continuous axial loading increased due to compression, whereas the stress of the fruit under continuous radial loading decreased due to tea seed slip. Radial loading was a more favourable loading mode for the fruit. The results could be useful to design an efficient shelling device for the *C. oleifera* fruit.

Author Contributions: Conceptualization, W.H. and X.W.; validation, P.L. and X.C.; writing—original draft preparation, X.C.; writing—review and editing, X.W.; funding acquisition, W.H. All authors have read and agreed to the published version of the manuscript.

Funding: This research was funded by Natural Science Foundation of Fujian Province (2020J01578).

Data Availability Statement: The data presented in this study are available on request from the corresponding author. The data are not publicly available due to some data is related the patent which is still in application.

Acknowledgments: We thank Dengfei Jie for the suggestion during the writing and contribution. We also thank the editor and reviewers for their helpful feedback to improve the paper. The authors gratefully acknowledge the financial support provided by the Natural Science Foundation of Fujian Province (2020J01578).

Conflicts of Interest: The authors declare no conflict of interest.

References

1. Wu, H.; Li, C.; Li, Z.; Liu, R.; Zhang, A.; Xiao, Z.; Ma, L.; Li, J.; Deng, S. Simultaneous extraction of oil and tea saponin from Camellia oleifera Abel. seeds under subcritical water conditions. *Fuel. Process. Technol.* **2018**, *174*, 88–94. [CrossRef]
2. Wang, Q.; Chang, S.; Tan, Y.; Hu, J. Mesopore structure in Camellia Oleifera shell. *Protoplasma* **2019**, *256*, 1145–1151. [CrossRef] [PubMed]
3. Hu, J.; Shi, Y.; Liu, Y.; Chang, S. Anatomical structure of Camellia oleifera shell. *Protoplasma* **2018**, *255*, 1777–1784. [CrossRef] [PubMed]
4. da Silva Ramos, C.A.; Soares, T.L.; Barroso, N.S.; Pelacani, C.R. Influence of maturity stage on physical and chemical characteristics of fruit and physiological quality of seeds of *Physalis angulata* L. *Sci. Hortic-Amst.* **2021**, *284*, 110124. [CrossRef]
5. Huang, W.; Wang, D.; Taylor, A. Seed pressing to remove cupules and obtain caryopses in eastern gamagrass. *Seed Sci. Technol.* **2016**, *44*, 114–124. [CrossRef]
6. Swami, S.B.; Thakor, N.S.J.; Gawai, A.M. Mechanical Properties of Cashew Nut Under Compression Loading at Varied Moisture Contents. *Agric. Res.* **2018**, *7*, 347–359. [CrossRef]
7. Rasli, A.M.M.; Nawi, N.M.; Ahmad, D.; Yahya, A. The effect of crop parameters on mechanical properties of oil palm fruitlets. *Sci. Hortic.-Amst.* **2019**, *250*, 352–358. [CrossRef]
8. Carcel, L.; Bon, J.; Acuña, L.; Nevares, I.; Del Alamo, M.; Crespo, R. Moisture dependence on mechanical properties of pine nuts from *Pinus pinea* L. *J. Food Eed.* **2012**, *110*, 294–297. [CrossRef]
9. Yang, X.; Qi, Y. Study on breaking mechanism of chestnut shell based on finite element analysis. *J. Phys. Conf. Ser.* **2021**, *1865*, 032001. [CrossRef]
10. Celik, H.K. Explicit dynamics simulation of Pecan fruit deformation under compressive loading—Part-2: Explicit dynamics simulation procedure. *J. Food Eed.* **2017**, *40*, e12582.
11. Celik, H.K. Non-linear FEM Based Compression Simulation of Pecan Fruit Kernels. *Akad. Gıda* **2016**, *14*, e12582. [CrossRef]
12. Celik, H.K. Explicit dynamics simulation of Pecan fruit deformation under compressive loading—Part-1: Determination of modulus of elasticity. *J. Food End.* **2017**, *40*, e12581. [CrossRef]
13. Cao, C.; Jiang, L.; Wu, C. Design and test on hammerhead of pecan shell-breaking machine [J/OL]. *Trans. Chin. Soc. Agric. Mac.* **2017**, *48*, 307–315. [CrossRef]
14. Bao, X.; Chen, B.; Dai, P.; Li, Y.; Mao, J. Crack Initiation Mechanism and Crack Analysis of Walnut. *Chem. Proc.* **2022**, *4*, 339. [CrossRef]
15. Fornés Comas, J.; Socias i Company, R.; Alonso Segura, J.M. Shell hardness in almond: Cracking load and kernel percentage. *Sci. Hortic-Amst.* **2019**, *245*, 7–11. [CrossRef]
16. Wu, D.; Yang, J.; Liu, Y.; Zhao, E.; Liu, L.; Cao, C. Research progress and trend of camellia fruit picking equipment in China. *J. Chin. Agric. Mech.* **2022**, *43*, 186–194. [CrossRef]
17. Lan, F.; Su, Z.; Li, Z.; Xie, S. Design and test on shelling and sorting machine of Camellia oleifera fruit. *Trans. Chin. Soc. Agric. Eng.* **2012**, *28*, 33–39. [CrossRef]
18. Wang, Q.; Hu, J.; Yang, T.; Chang, S. Anatomy and lignin deposition of stone cell in Camellia oleifera shell during the young stage. *Protoplasma* **2021**, *258*, 361–370. [CrossRef]
19. Jin, Q.; Yan, C.; Qiu, J.; Zhang, N.; Lin, Y.; Cai, Y. Structural characterization and deposition of stone cell lignin in Dangshan Su pear. *Sci. Hortic.-Amst.* **2013**, *155*, 123–130. [CrossRef]
20. Stelte, W.; Holm, J.K.; Sanadi, A.R.; Barsberg, S.; Ahrenfeldt, J.; Henriksen, U.B. A study of bonding and failure mechanisms in fuel pellets from different biomass resources. *Biomass. Bioenerg.* **2011**, *35*, 910–918. [CrossRef]
21. Borrero-Lopez, A.M.; Valencia, C.; Dominguez, G.; Eugenio, M.E.; Franco, J.M. Rheology and adhesion performance of adhesives formulated with lignins from agricultural waste straws subjected to solid-state fermentation. *Ind. Crop. Prod.* **2021**, *171*, 113876. [CrossRef]

Disclaimer/Publisher's Note: The statements, opinions and data contained in all publications are solely those of the individual author(s) and contributor(s) and not of MDPI and/or the editor(s). MDPI and/or the editor(s) disclaim responsibility for any injury to people or property resulting from any ideas, methods, instructions or products referred to in the content.